Journal of Analytical and Applied Pyrolysis 105 (2014) 317–326

Contents lists available at ScienceDirect

Journal of Analytical and Applied Pyrolysis

journal homepage: www.elsevier.com/locate/jaap

Investigation on flame retardancy, combustion and pyrolysis behavior of flame retarded unsaturated polyester resin with a star-shaped phosphorus-containing compound

Zhiman Bai[a,c], Lei Song[a], Yuan Hu[a,c,*], Xinglong Gong[a,b,**], Richard K.K. Yuen[c,d]

[a] State Key Lab of Fire Science, University of Science and Technology of China, 96 Jinzhai Road, Hefei, Anhui 230026, People's Republic of China
[b] CAS Key Laboratory of Mechanical Behavior and Design of Materials, Department of Modern Mechanics, University of Science and Technology of China, People's Republic of China
[c] USTC-CityU Joint Advanced Research Centre, Suzhou Key Laboratory of Urban Public Safety, Suzhou Institute for Advanced Study, University of Science and Technology of China, 166 Ren'ai Road, Suzhou, Jiangsu 215123, People's Republic of China
[d] Department of Civil and Architectural Engineering, City University of Hong Kong, Tat Chee Avenue, Kowloon, Hong Kong

ARTICLE INFO

Article history:
Received 4 June 2013
Accepted 21 November 2013
Available online 1 December 2013

Keywords:
Unsaturated polyester resin
Thermal degradation
Pyrolysis: evolved gas analysis
Flame retardancy

ABSTRACT

The phosphorus-containing star-shaped flame retardant (TRIPOD-DOPO) was synthesized, while the flame retardant unsaturated polyester resins (FR-UPRs) composites with various amounts of TRIPOD-DOPO were prepared. The thermogravimetric analysis (TGA) and oxygen index (OI) results showed that the incorporation of TRIPOD-DOPO improves the thermal stability and flame retardancy of UPR. The combustion properties of composites were evaluated by microscale combustion calorimeter (MCC), and the results indicated that TRIPOD-DOPO decreased the peak heat release rate (pHRR) and total heat release (THR) of UPR. Fourier transform infrared coupled with the thermogravimetric analyzer (TG–IR) revealed that UPR and TRIPOD-DOPO decomposed independently of each other. Flame inhibition was expected to occur in the gas phase. Under the air condition, TRIPOD-DOPO showed a more obviously condensed phase interaction increasing charring from the TG results. The SEM results showed that the residual char of composites were more compact and continuous, which could prevent mass and thermal transfer.

1. Introduction

Unsaturated polyester resin (UPR) are prepared by reaction of aliphatic diols with unsaturated and saturated diacids, and diluted with unsaturated co-reactant diluents like styrene [1]. UPR are widely used as resin components in composites for the building industry, transportation sector, and electrical industry, in boats and others, because of their low cost, easy processability, low densities, good corrosion resistance, and high strength-to-weight ratios. The cross-linking reactions of unsaturated polyesters include radical polymerizations between a pre-polymer that contains unsaturated groups and styrene [2,3]. Unfortunately, due to their intrinsic chemical composition and molecular structures, typical unsaturated polyester resins are highly flammable, and produce large quantities of smoke and toxic gases when burnt.

Although halogen atoms (such as bromine and chlorine) form the most widely applied flame retardant materials, the European Community (EC) has proposed to restrict the use of halogen flame retardants because highly toxic smoke and severe environmental pollution may be produced during combustion [4]. Consequently, in order to protect the environment and human's health, researchers have focused on exploiting environmental friendly halogen-free flame retardants for UPR. It is reported that UPR can be modified with hydroxide [5], ammonium polyphosphate, melamine pyrophosphate [6], layer double hydroxide [7], and montmorillonite [8] to enhance their flame retardancy.

Recently, phosphorus-containing compounds, as halogen-free flame retardant, have received considerable attention [9–11]. Thus 9,10-dihydro-9-oxa-10-phosphaphe-nanthrene-10-oxide (DOPO) has became one of the most important flame retardants in this field, now used in several modification as a reactive or additive compound [12–14]. DOPO can either act only in the gas phase (via flame inhibition), or in the gas phase and in the condensed phase (via char formation) at the same time [15,16]. Moreover, nitrogen compounds have also been known for their good flame-retardant properties combined with excellent thermal and chemical

* Corresponding author at: State Key Lab of Fire Science, University of Science and Technology of China, 96 Jinzhai Road, Hefei, Anhui 230026, People's Republic of China. Tel.: +86 551 63601664; fax: +86 551 63601664.
** Corresponding author at: CAS Key Laboratory of Mechanical Behavior and Design of Materials, Department of Modern Mechanics, University of Science and Technology of China, People's Republic of China. Tel.: +86 551 63600419.
E-mail addresses: yuanhu@ustc.edu.cn (Y. Hu), gongxl@ustc.edu.cn (X. Gong).

0165-2370/$ – see front matter © 2013 Published by Elsevier B.V.
http://dx.doi.org/10.1016/j.jaap.2013.11.019

properties such as high thermal-oxidative resistance, low toxicity, etc. [17,18]. Although the oligomeric star-shaped DOPO based flame retardants have been used as effective flame retardants for epoxy [19–21], little attention has been focused on the application for UPR.

In this work, the phosphorus-containing star-shaped flame retardant TRIPOD-DOPO was synthesized, and the flame retardant UPR composites with TRIPOD-DOPO were prepared. The focus of this study lies on the influence of TRIPOD-DOPO on the flame retardant properties, on the pyrolysis analysis and on the combustion properties of thermosets were investigated.

2. Experimental

2.1. Materials

Unsaturated polyester resin (commercial grade, type 196#) was kindly supplied by Heifei Chaoyu Chemical Co. Ltd (Anhui, China). Cyanuric chloride was supplied by Alfa-Aesar Chemistry Industry Co. Ltd. 9,10-Dihydro-9-oxa-10-phosphaphenanth-re-ne-10-oxide (DOPO) was provided by Shandong Mingshan Fine Chemical Industry Co. Ltd (Shandong, China). 4-Hydroxybenzaldehyde (p-HBD), sodium carbonate anhydrous (Na_2CO_3), sodium sulfate anhydrous (Na_2SO_4), benzoyl peroxide (BPO), benzene, ethyl acetate and toluene were all reagent grade and purchased from Sinopharm Chemical Reagent Co. Ltd (Shanghai, China). BPO was purified by recrystalizaiton, and other reagents used directly without purifying.

2.2. Synthesis of 2,4,6-tris(p-formylphenoxy)-1,3,5-triazine (TRIPOD)

The TRIPOD was synthesized by the method described in the previous report [22]. The synthesis route is shown in Scheme 1. A 500 ml three-neck and round-bottom glass flask equipped with a mechanical stirrer, a circumference condenser and thermometer was charged with 50 g of Na_2CO_3 and 250 ml of benzene. Then 8.0 g p-hydroxybenzaldehyde and 3.0 g cyanuric chloride were added to the above suspension. The mixture was refluxed at 80 °C for 24 h. The reaction mixture was then cooled and the solid was removed by filtration and washed with hot ethyl acetate twice. The filtrate was extracted with 10% Na_2CO_3 twice and H_2O once. The organic layer was dried with anhydrous Na_2SO_4 and then concentrated. The white powder was recrystallized from ethyl acetate to obtain a white fluffy precipitate.

2.3. Synthesis of TRIPOD-DOPO

11.03 g TRIPOD, 16.20 g DOPO and 300 ml of toluene were charged into a 500 ml round-bottom flask. The mixture was stirred and heated at 110 °C for 5 h under the protection of nitrogen. Thereafter, the product was obtained by the filtration and the filtered precipitant was washed with toluene. Finally, the product was dried in vacuum at 60 °C to give a white powder.

2.4. Preparation of UPR/TRIPOD-DOPO composites

UPR and required amounts of TRIPOD-DOPO were charged into a 100 ml three-necked round bottom flask equipped with a mechanical stirrer. The mixture was stirred thoroughly until a homogeneous mixture was obtained at room temperature. Thereafter, 2 wt% radical initiator BPO as UPR amount was added and used to initiate the curing reaction with vigorous stirring for another 20 min. After the mixture was de-aerated under vacuum for 5 min, the casting composition was poured into Teflon molds. The reaction mixtures were cured at 70 °C for 4 h and post-cured at 120 °C for 3 h. Finally, samples were cooled to room temperature. The formulation of UPR/TRIPOD-DOPO composites was listed in Table 1.

2.5. Measurements

2.5.1. Structural characterization of TRIPOD-DOPO

All ^1H NMR spectra were performed on a Bruker AV400 NMR spectrometer (400 MHz) operating in the Fourier transform mode using DMSO-d_6 and $CDCl_3$ as solvent.

The Fourier transform infrared (FTIR) spectra were recorded using a Nicolet 6700 spectrophotometer in KBr pellets. Spectra in the optical range of 500–4000 cm^{-1} were obtained by averaging 16 scans at a resolution of 4 cm^{-1}.

Molecular weight of TRIPOD-DOPO was determined by mass spectrometer of EXPASY/Protein Prospector in DMSO.

2.5.2. Thermogravimetric analysis (TGA)

The TGA was carried out on a TGA Q5000 IR thermalgravimetric analyzer (TA Instruments). About 5 mg of sample was heated from room temperature to 800 °C at a heating rate of 10 °C/min under both nitrogen and air condition. The temperature reproducibility of the instrument is ±1 °C, while the mass reproducibility is ±0.2 wt%.

2.5.3. Thermogravimetric analysis/infrared spectrometry (TG–IR)

The TG–IR of the cured sample was carried out by using the TGA Q5000 IR thermogravimetric analyzer, which was interfaced to the Nicolet 6700 FTIR spectrophotometer. About 5.0 mg of the sample was put in an alumina crucible and heated from room temperature to 700 °C at the heating rate of 20 °C/min in nitrogen atmosphere.

2.5.4. Microscale combustion calorimetry (MCC)

The MCC tests were carried out on a Govmark MCC-2 microscale combustion calorimeter, which was used to investigate the combustion of the cured samples. According to the standard of ASTM D7309-07, about 4 mg cured samples were heated to 700 °C at a heating rate of 1 °C/min and in a stream of nitrogen flowing at 80 cm^3/min. Next, the pyrolysis products were mixed with oxygen (20 ml/min) entering a 900 °C combustion furnace and the heat of combustion of the pyrolysis products were measured by the oxygen consumption principle. The experimental error is ±3%.

2.5.5. The oxygen index (OI)

The OI values were measured on a HC-2 oxygen index meter (Jiangning Analysis Instrument Co., China). According to ISO 4589-2, the specimens used for the test were of dimensions 100 mm × 6.5 mm × 3 mm. The specimens belonged to the form IV type material sample in the standard, and they were ignited using top surface ignition method. It should be taken into account that OI test is under the controlled laboratory conditions, and the results obtained are dependent upon the shape, orientation of the test specimen and the ignition mode, which cannot used to describe or appraise the fire hazard under actual fire condition.

2.5.6. Underwriter Laboratories 94 vertical burning test (UL-94)

The UL-94 was performed using vertical burning instrument (CFZ-2-type, Jiangning Analysis Instrument Company, China) and the specimens for test were of dimensions of 130 mm × 13 mm × 3 mm. In the measurement, the samples were vertically exposed to a Bunsen burner flame for 10 s. If the samples were self-extinguished, another 10 s was employed. The classification of the samples was defined according to ISO 1210.

2.5.7. Morphology of residual char

Scanning electron microscopy (SEM) images were obtained with a Hitachi X650.

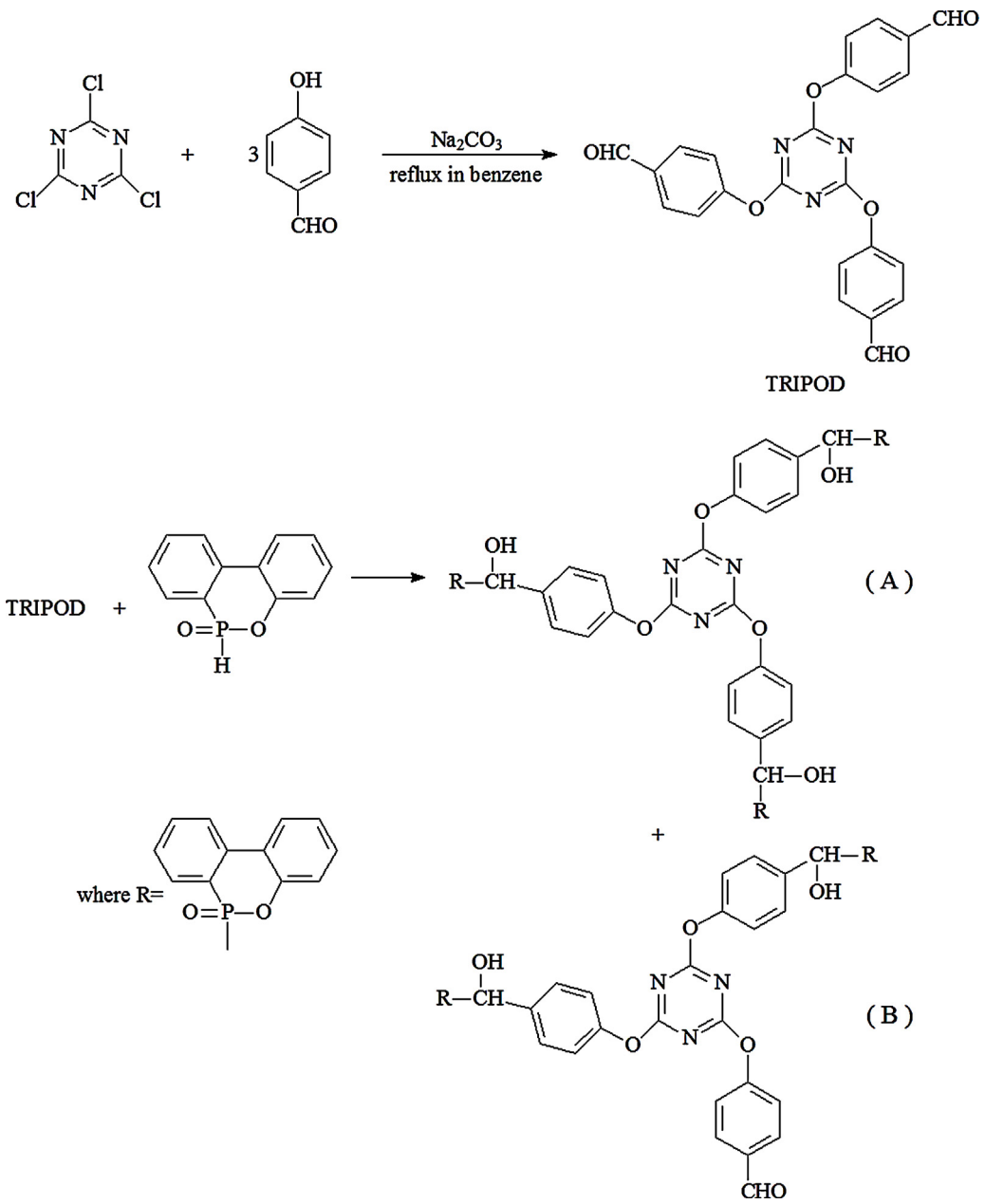

Scheme 1. Synthesis route of TRIPOD and TRIPOD-DOPO.

3. Results and discussion

3.1. Structure characterization

TRIPOD-DOPO was synthesized by the reaction between TRIPOD and DOPO, as shown in Scheme 1. Their structures were characterized by NMR, Mass and FTIR. As can be seen from Fig. 1(a), as for TRIPOD, the chemical shifts at 7.31 ppm and 7.91 ppm are attributed to $-CH_2$ of aromatic ring, while the –CHO resonance appears at 9.99 ppm. In the case of TRIOD-DOPO, aromatic signals from p-HBD and DOPO appear at 7.08–8.23 ppm and 6.28–6.50 ppm. Moreover, the appearances of characteristic peaks at 5.19 ppm and 5.38 ppm correspond to –CH confirms the addition reaction between TRIPOD and DOPO. However, the –CHO peak at 9.99 ppm indicates that the addition reaction was not completed fully. Fig. 1(b) shows the ^{31}P NMR spectrum of TRIPOD-DOPO; there are two peaks at 30.94 ppm and 14.45 ppm attributed to the two structures, respectively. This is also confirmed by mass result as

Table 1
The composition and results of UL-94, OI tests for UPR and FR-UPR composites.

Sample	UPR (g)	BPO (g)	DOPO-TRIPOD (g)	DOPO-TRIPOD percentage (wt%)	OI value (%)	UL-94
UPR	30	0.6	0	0	20.5 ± 0.5	No vertical rating
UPR-1	27	0.6	3	10	24.0 ± 0.5	No vertical rating
UPR-2	24	0.6	6	20	26.0 ± 0.5	V-2
UPR-3	21	0.6	9	30	30.5 ± 0.5	V-0

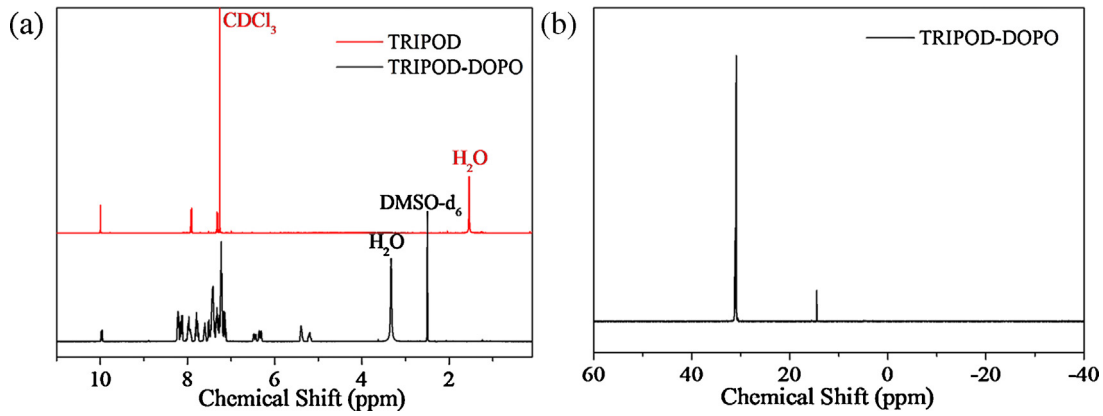

Fig. 1. ^{1}H NMR (a) spectra of TRIPOD, TRIPOD-DOPO and ^{31}P NMR (b) spectrum of TRIPOD-DOPO.

Fig. 2 shown, it can be seen that m/z = 1089.88 and 873.88 corresponds to AH+ and BH+, respectively.

Fig. 3 shows the FTIR spectra of TRIPOD and TRIPOD-DOPO. As for TRIPOD, the significant absorption corresponding to C—H and C=O absorption of aldehyde group are observed at 2840 cm^{-1} and 1703 cm^{-1}, respectively. The absorptions at 1600 cm^{-1} and 1497 cm^{-1} are attributed to the aromatic vibration. Meanwhile, the absorption at 1570 cm^{-1} is assigned to triazine ring stretching absorption. Furthermore, the absorptions at 1213 cm^{-1} and 1162 cm^{-1} are attributed to C—O—Ph. All the above confirms the structure of TRIPOD. In the case of TRIPOD-DOPO, the new absorption peaks at 1140 cm^{-1}, 1017 cm^{-1}, 925 cm^{-1}, are attributed to P—O—C, P=O, P—Ph, respectively, which confirm the presence of DOPO structure. Compared to TRIPOD, the absorption at 1703 cm^{-1} corresponding to aldehyde group of TRIPOD-DOPO is very weak indicating that the structure A is major in the product. All the information above confirms the formation of the structure shown in Scheme 1.

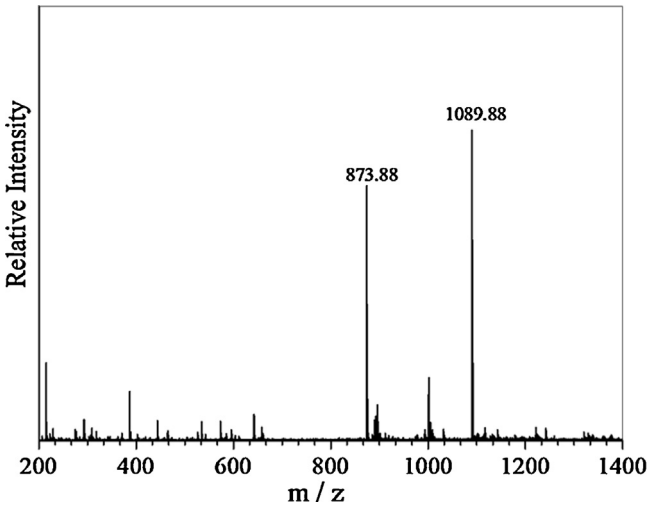

Fig. 2. Mass spectrum of TRIPOD-DOPO.

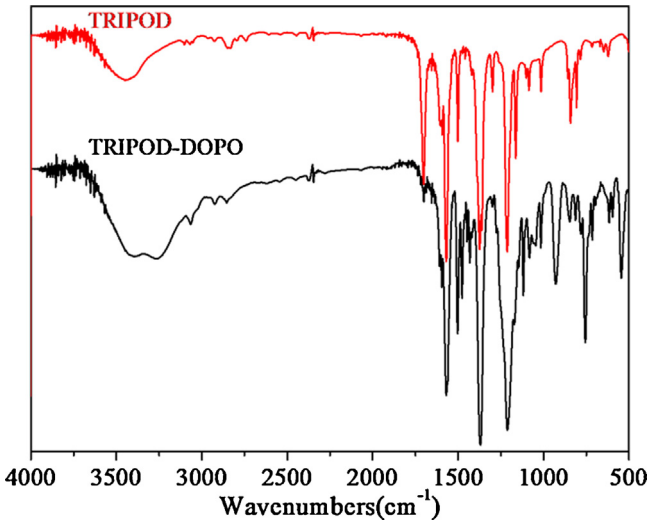

Fig. 3. FTIR spectra of TRIPOD and TRIPOD-DOPO.

3.2. Thermal degradation

The thermal degradation behaviors of UPR and FR-UPR composites were assessed by the thermogravimetic analysis (TGA) under both air and nitrogen atmosphere. The TGA and derivative thermogravimetric (DTG) curves are given in Figs. 4 and 5, while detailed TGA data are presented in Table 2. The onset degradation temperature (T_d) is considered as the temperature at which the weight loss was approximately 5%. The solid residual char at 600 °C is obtained from the TG curves; the temperatures of the maximum weight loss rate (T_{max}) of samples are obtained from the DTG curves.

UPR displays three main steps of degradation in air [23]. As shown in Fig. 4, the thermal oxidative degradation process of UPR has three steps. The first step is in the temperature range of 250–300 °C corresponding to a loss of water by dehydration, however, no obvious peak founded on DTG curves due to the little mass loss of this step. The main degradation step ranging from 300 to 430 °C results from the chain scission of polystyrene and polyester fragments corresponding to a strong DTG peak at 394 °C. This leads to the formation of a primary carbonaceous char, which degraded at high temperature around 540 °C of the third step.

Fig. 4(a) and (b) also shows TG and DTG curves of the FR-UPRs in air. The thermal oxidative degradation processes of FR-UPRs have

Table 2
TGA data of UPR and FR-UPR composites in both air and nitrogen atmosphere.

Sample	$T_d \pm 1$ (°C)		$T_{max} \pm 1$ (°C)		Char at 600 °C ± 0.2 (wt%)	
	Air	N_2	Air	N_2	Air	N_2
UPR	250	237	394	393	0.18	8.16
UPR-1	223	218	410	403	2.63	4.81
UPR-2	228	238	404	402	7.93	9.07
UPR-3	241	217	396	398	14.46	8.58

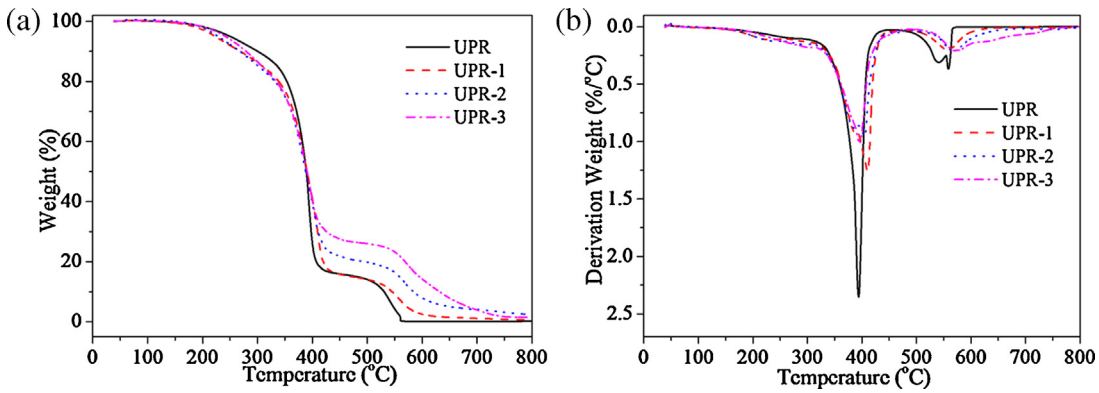

Fig. 4. TG (a) and DTG (b) curves of UPR composites in air atmosphere.

the similar three stages as the pristine UPR; however, the degradation was substantially altered by incorporation of TRIPOD-DOPO into UPR. Compared the T_d for UPR at 250 °C, FR-UPRs decompose earlier than pure UPR at lower temperature. This is in accordance with the behavior of phosphorus-based flame retardants as reported previously [24], suggesting low degradation temperature of the relative weak P—O—Ph chemical bond in TRIPOD-DOPO molecular structure. The reduction in T_d is also attributed to the lower crosslinking density of the systems due to the replacement of 30 wt% of UPR by nonreactive flame retardant [21]. However, T_{max} of FR-UPRs are slightly higher than that of pure UPR with the decreased maximum mass loss rate, indicating that FR-UPRs decompose slowly than pure UPR. As the TRIPOD-DOPO content increases, the FR-UPRs show higher thermal stability beyond 400 °C, and the residue left at 600 °C increases significantly. The char yield at 600 °C for UPR-3 is 14.46 wt% which is much higher than 0.18 wt% of UPR. The formed char will limit the release of combustible gases and decrease the thermal conductivity of the burning materials, and this will consequently retard the flammability of the materials. TG results under air condition indicate that the incorporation of TRIPOD-DOPO improves the thermal stability of FR-UPR, promotes the formation of char residue.

When the samples were evaluated in nitrogen, their degradation behaviors display differently from those in air. It is obvious that replacing air by a non-oxidative atmosphere affects the thermal degradation behaviors of samples, as Fig. 5 illustrates. The thermal degradation processes of samples consist of two steps. Compared to the thermal oxidative degradation process in the air atmosphere, the third decomposition step around 540 °C, which is due to the further char oxidation decomposition, disappears in nitrogen. The first decomposition stage ranging from 195 to 320 °C is ascribed to the water by dehydration and decomposition of TRIPOD-DOPO, which can be confirmed by the fact that as the TRIPOD-DOPO content increases, the DTG peaks of this stage become more obvious. The second decomposition stage ranging from 320 to 500 °C corresponds to the chain scission of polystyrene and polyester fragments with the DTG peaks around 400 °C. It can be seen from Fig. 5, the T_d of FR-UPRs decreases as the TRIPOD-DOPO content increases, which is similar to the results in the air atmosphere. However, T_{max} of FR-UPR is slightly higher than that of pure UPR with the decreased maximum mass loss rate. It is found that the char residue at 600 °C for UPR-2 and UPR-3 are 9.07 and 8.58 wt%, respectively, slightly higher than the values of 8.16 wt% for pure UPR. The char yield of UPR-3 under nitrogen and air atmosphere are 8.58 and 14.46 wt%, respectively, and this demonstrates that the presence of oxygen has an accelerating effect on acid-catalyzed cross-linking actions in the polymer degradation [25]. Phosphates are well known to enhance charring production because of phosphoric acid formation. DOPO could form relative weaker phosphonic acid instead of phosphoric acid. The weaker acid would be less effective at promoting (acid-catalyzed) char formation in the polymer. This is consistent with the reduced char residue in nitrogen atmosphere. The greater increase in the residue under air condition might be due to the oxidation of phosphonic acid to phosphoric acid in the polymer.

The summary of TGA and DTG results indicate that the incorporation of TRIPO-DOPO into UPR causes the lower onset thermal degradation temperature. However, it could enhance the char yields and decrease the decomposition rate. More significant is the difference between nitrogen and air atmosphere observed for the char yields, indicating that the presence of oxygen has a dramatic effect on the char formation of FR-UPRs. The formed char can act as a mass transport barrier and an insulator between the polymer matrix and the surface where the degradation occurs. Generally,

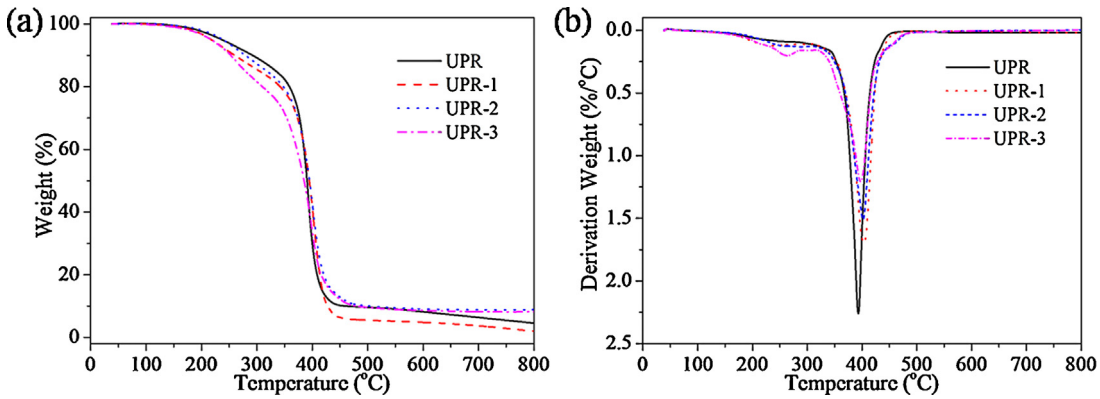

Fig. 5. TG (a) and DTG (b) curves of UPR composites in nitrogen atmosphere.

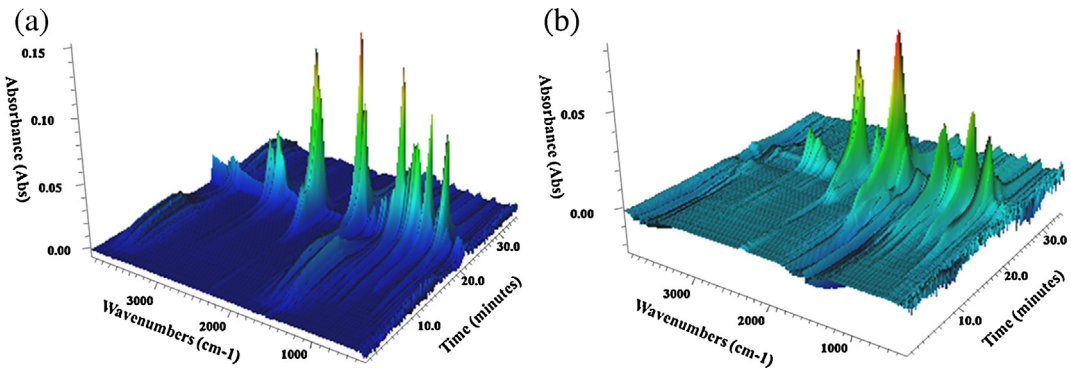

Fig. 6. The 3D surface graph for the FTIR spectra of the evolved gases produced by UPR (a) and UPR-3 (b).

the FR-UPRs reveal enhanced thermal stability and char formation in comparison with neat UPR under both nitrogen and air condition.

3.3. Pyrolysis: evolved gas analysis

TG–IR was used to analyze the gaseous products during the thermal degradation. The 3D TG–IR spectra of gas phase in the thermal degradation of UPR and UPR-3 are shown in Fig. 6(a) and (b), respectively. Peaks in the regions 3500–3700 cm^{-1}, 2730–3150 cm^{-1}, 2400–2300 cm^{-1}, 1869–1807 cm^{-1} and 1743–1104 cm^{-1} are noted. Some of the gaseous decomposition products of UPR materials are proved unambiguously by characteristic strong FTIR signals. The FTIR spectra of evolved gases in the above mentioned temperature range shows the degradation products contain CO_2 (2400–2300 cm^{-1}), CO (2300–2100 cm^{-1}), ester (1743, 1265 cm^{-1}), hydrocarbons (2950–2850 cm^{-1}) and anhydride (1869–1870 cm^{-1}) [26].

FTIR spectra of pyrolysis products of UPR and UPR-3 at the maximum release rate and corresponding DTG curves are shown in Figs. 7 and 8, respectively. As can be seen from Fig. 7, UPR undergoes one step degradation with a strong DTG peak at 400 °C, and the main products of the UPR are compounds containing –OH (such as H_2O, phenol; 3500–3800 cm^{-1}), CO_2 (2359 cm^{-1}), hydrocarbons (2947–2800 cm^{-1}), ester (1743, 1265, 1104 cm^{-1}), anhydride

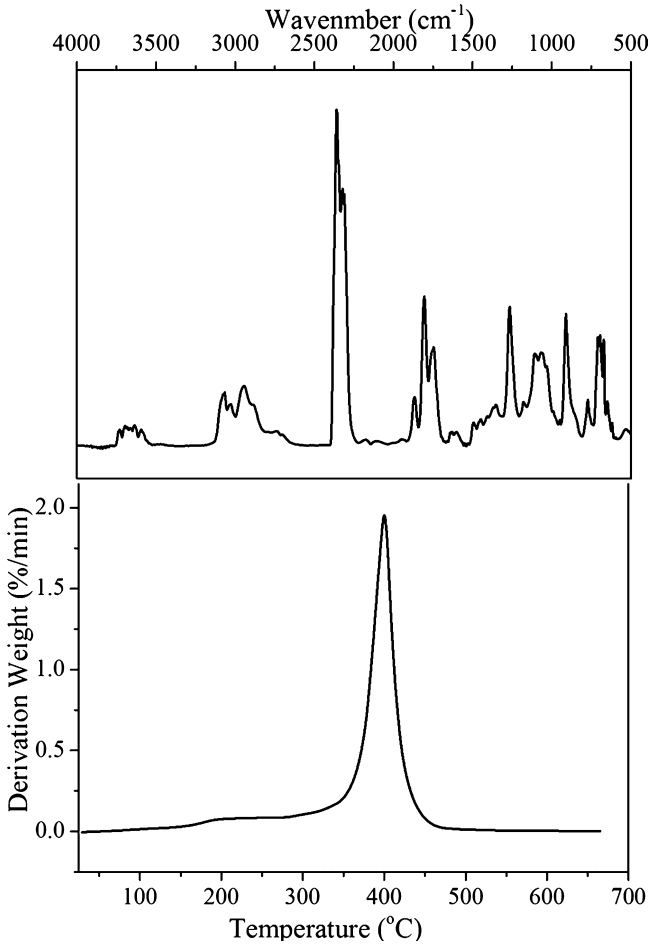

Fig. 7. FTIR spectra of pyrolysis products of UPR at the maximum release rate and corresponding DTG curve.

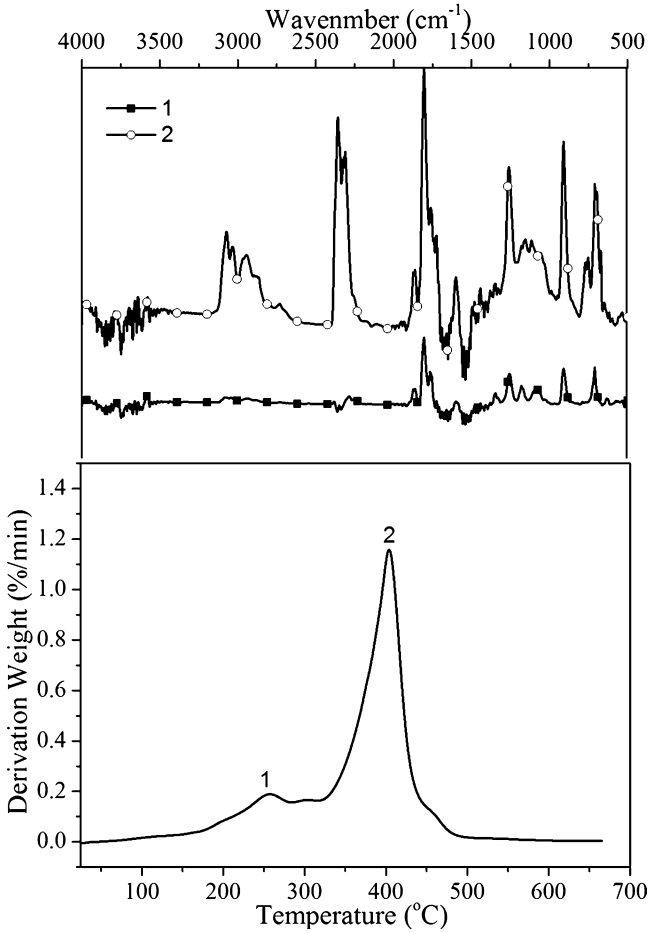

Fig. 8. FTIR spectra of pyrolysis products of UPR-3 at the maximum release rate and corresponding DTG curve.

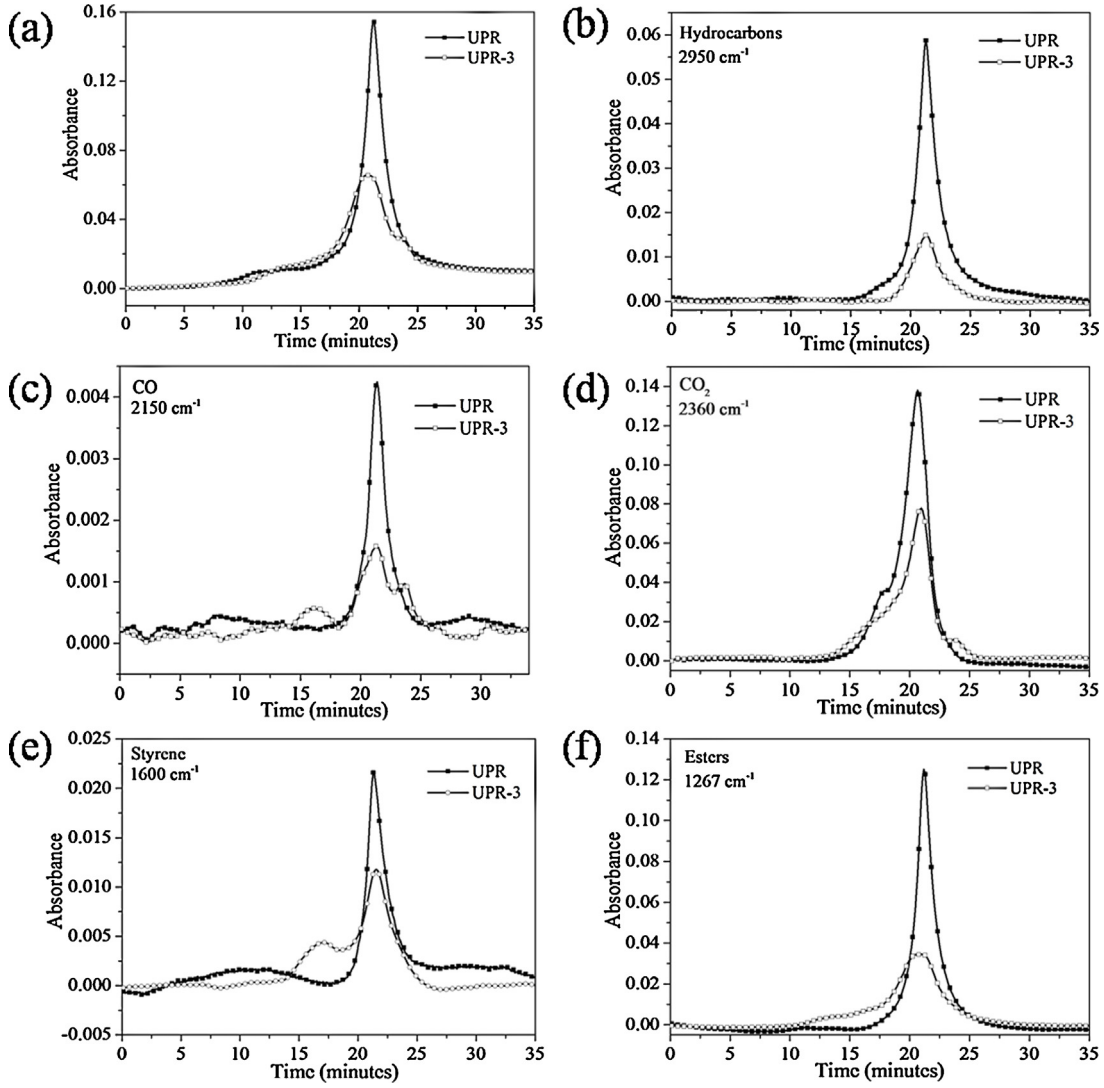

Fig. 9. Absorbance of pyrolysis products for UPR and UPR-3 vs. time: (a) total release, (b) hydrocarbons, (c) CO, (d) CO_2, (e) styrene and (f) esters.

(1869, 1807, 909 cm^{-1}) and styrene (1600 cm^{-1}). All the compounds are consistent with the previous results by Kandare et al. [23]. It is well-known that depolymerization is the main process associated with the thermal degradation of polymers. It is proposed that UPR firstly undergoes chain scission of polystyrene and polyester segments, which releases styrene and anhydride, followed by the further degradation at high temperature to produce low molecular compounds such as CO, CO_2 and hydrocarbons, etc. This degradation process is also verified by TG. However, UPR-3 possesses two DTG peaks at 257 and 403 °C, respectively. Compounds containing phosphorus, such as P=O at 1257 cm^{-1}, P—O—C at 1080 and 905 cm^{-1} were observed on the curve 1 in Fig. 8, indicating that the former DTG peak is mainly due to the decomposition of TRIPOD-DOPO, and flame inhibition based on gas phase flame retardant mechanism is expected to occur. The similar products with pure UPR were obtained on the curve 2 of UPR-3, which means that adding TRIPOD-DOPO to the UPR did not change the main kinds of decomposition products.

In order to clearly understand the change of these products, the relationship between intensity of characteristic peak and time for volatilized CO, CO_2, styrene, esters, hydrocarbons as well as the total release, respectively, are illustrated in Fig. 9. It can be found that the absorbance intensity of pyrolysis products and total release of UPR-3 is much lower than that of pure UPR. This is due to combustible UPR was replaced by flame retardant; and phosphoric acid produced by decomposition by TRIPOD-DOPO reacts with UPR matrix, resulting in the reduction of volatilized products and enhancement of residual char. Meanwhile, the char layer becomes a barrier to the gas products leading to the reduced intensity. Moreover, the MMLR of UPR-3 is much lower than that of UPR under nitrogen condition, which also causes the reduction of intensity.

The summary of TG–IR results under nitrogen show that the incorporation of TRIPOD-DOPO divide the decomposition stage of UPR-3 into two obviously stage. A major portion of the TRIPOD-DOPO was decomposed in the gas phase at the former stage, and the UPR matrix decomposed at the latter stage. The TRIPOD-DOPO did not change the kinds of decomposed gaseous products of UPR, but it could reduce their release intensity.

3.4. Combustion properties

The Microscale Combustion Calorimeter (MCC) has become one of the most effective methods for investigating the combustion properties of polymer materials [27–29]. The MCC uses oxygen consumption calorimetry to measure the rate and amount of heat. The heat is produced by complete combustion of the fuel gases generated during controlled pyrolysis of a milligram sized sample.

Table 3
MCC data of UPR and FR-UPR composites.

Sample	pHRR	THR	Temperature
UPR	457.9	19.7	400.1
UPR-1	343.1	16.6	410.0
UPR-2	286.0	16.2	408.2
UPR-3	218.9	14.3	399.5

pHRR: peak heat release rate (W/g); THC: total heat of combustion (kJ/g); T_{max}: Temperature of maximum heat release rate (°C).

The heat release rates (HRRs) curves of samples are shown in Fig. 10, and the corresponding combustion data are presented in Table 3. The incorporation of TRIPOD-DOPO into the UPR obviously decreases the pHRR. Pure UPR gives the highest pHRR of 457.9 W/g, while the UPR-3 gives much lower pHRR of 218.9 W/g. It is reported that there are two main factors that can determine the pHRR: maximum mass loss rate (MMLR) and the heat of combustion of the decomposition product [30]. In agreement with results received in TG–IR it is concluded that combustion tests are influenced by gas phase mechanism. In this case, hydrogen and hydroxyl radicals are rendered harmless by radical recombination in the gas phase. Meanwhile the combustible UPR material was replaced by a sufficient amount of inert flame retardant. Both of them lead to the reduced heat release of combustion. Furthermore, the incorporation of TRIPOD-DOPO decreases the MMLR and the release intensity of evolved gas products. As a result, the pHRR of UPR-3 decreases by 52.2% in comparison with that of UPR. THR, calculated from the total area under the HRR peaks, is another important parameter used to evaluate fire hazard. UPR and UPR-3 give THR values of 19.7 and 14.3 kJ/g, respectively, corresponding to about 27.4% reduction in the THR value of neat UPR. It can be found that the incorporation of TRIPOD-DOPO can reduce the pHRR and THR significantly.

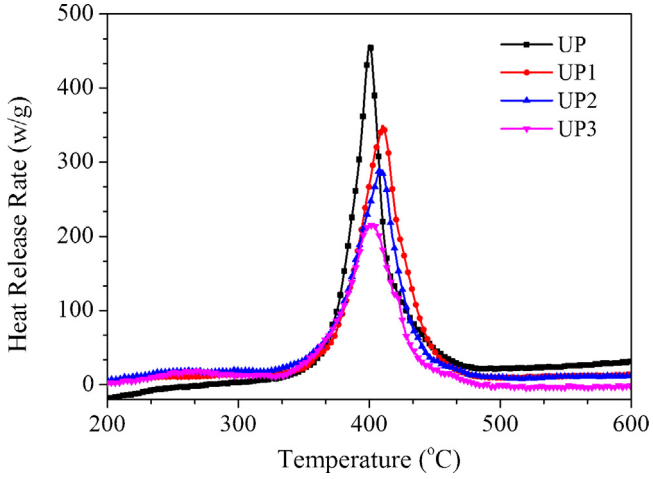

Fig. 10. The HRR curves of the UPR and FR-UPR composites at 1 K/s heating rate.

3.5. Flame-retardancy

OI and UL-94 vertical burning tests are widely used to evaluate the flammability of polymer materials [31]. The OI values and UL-94 testing rating of UPR and UPR composites are given in Table 1. UPR is a kind of flammable material with a low OI value of 20.5%, and shows no vertical rating in UL-94 test. As can be seen from Table 1, the higher OI values are obtained with increasing TRIPOD-DOPO loading. OI value increases drastically from 20.5% to 30.5% when TRIPOD-DOPO content is increased from 0 to 30 wt%. The experimental results of UL-94 show that the UPR-3 with 30 wt% TRIPOD-DOPO loading gives a V-0 rating. Both the OI and UL-94 results indicate that TRIPOD-DOPO exhibits good flame-retardant effect on UPR. TRIPOD-DOPO can act in the gas phase (via flame inhibition) and in the condensed phase (via char formation) at the same time. The char residue of samples at the end of OI test is shown in Fig. 11. It is obvious that there is almost no residue left at the end of OI test for pure UPR, whereas FR-UPRs are covered with char residue. The results demonstrate that TRIPOD-DOPO could promote the formation of char residue, which protect the material underneath from heat and hinders pyrolysis gas transport.

3.6. Morphology of residual char

The high quality char acts as an insulating barrier during degradation and this protective barrier can prevent the transfer of mass and heat between the gas and condensed phases. As a result, the morphology of the char residue could be a very important criterion when define the ability of a flame retardant [32]. In order to further investigate char morphology under the air condition, UPR and

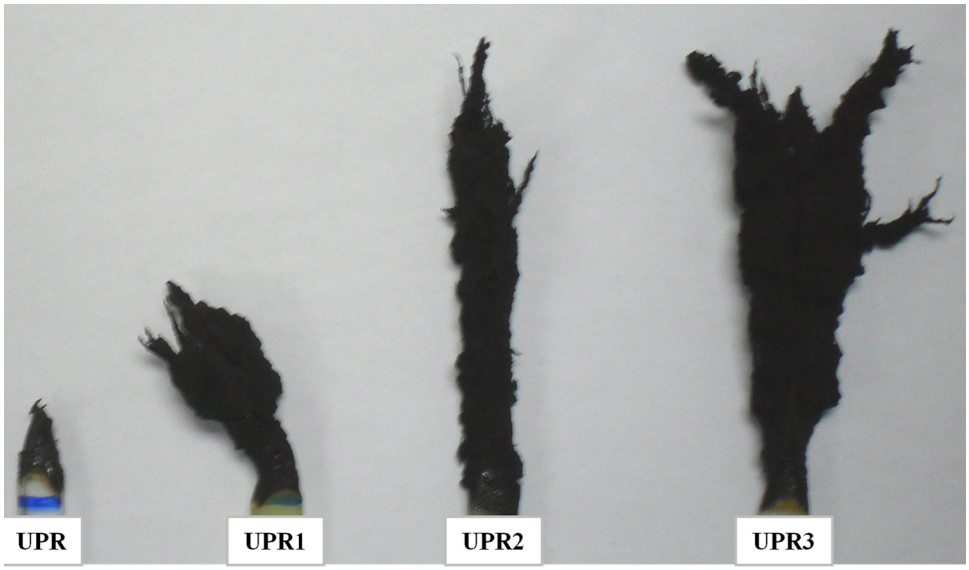

Fig. 11. Digital photos of the samples after OI test.

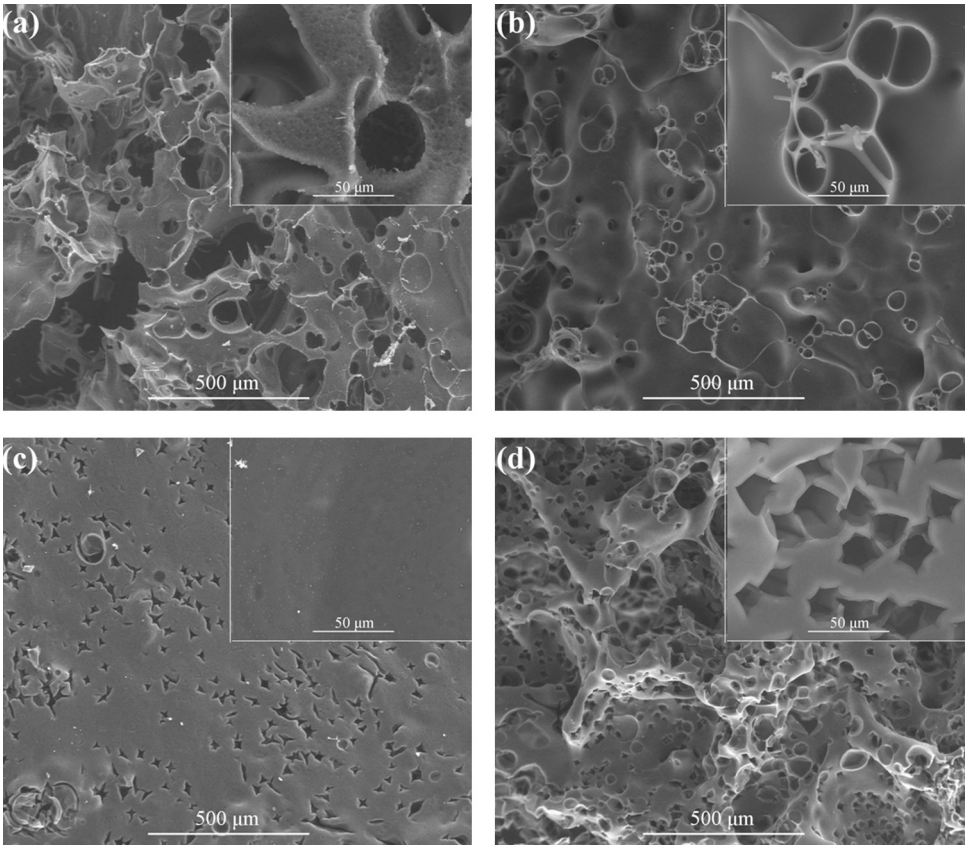

Fig. 12. SEM images of the outer char residue of (a) UPR, (c) UPR-3 and the inner residual char of (b) UPR and (d) UPR-3.

UPR-3 were pyrolyzed in a muffle furnace at 600 °C for 10 min, and then char was obtained. Fig. 12 presents the SEM micrographs of the char. As can be seen from Fig. 12(a) and (b) for UPR, loose and flaky char could be observed at the outer surface of UPR, with lots of large holes distributed on the surface. Meanwhile, the continuous char was formed in the interior part, with a few of holes and bubbles. Unlike the UPR morphology, the char residue of UPR-3 depicted in Fig. 11(c) and (d), exhibits a much more compact and smooth morphology. Moreover, a honeycomb-like char is observed within the char. The honeycomb-like char probably exhibits much better heat insulation and mechanical properties [32]. As a result, the honeycomb-like char of UPR-3 can significantly reduce the mass and energy transfer during combustion, and thus provide better flame shield for the underlying material and improve the flame retardancy of FR-UPR.

4. Conclusions

The phosphorus-containing star-shaped flame retardant (TRIPOD-DOPO) was successfully synthesized, and the structure was confirmed using ^{1}H NMR, ^{31}P NMR, Mass and FTIR. FR-UPR composites with various amounts of TRIPOD-DOPO were prepared. With 30 wt% TRIPOD-DOPO, the composites can reach the OI value of 30.5% and pass the UL-94 V-0 rating. Meanwhile the reduced pHRR and THR was observed from MCC results. All of above revealed that TRIPOD-DOPO can impart excellent flame retardant properties to UPR, and act in the gas phase (via flame inhibition) and in the condensed phase (via char formation) at the same time. The residual char of UPR-3 showed much more compact by comparison with UPR, and a honeycomb-like char was formed within the char.

Acknowledgements

This research was supported by the National Natural Science Foundation of China (no. 11125210 and no. 51036007), Specialized Research Fund for the Doctoral Program of Higher Education (20103402110006) and a grant from the Research Grant Council of the Hong Kong Special Administrative Region, China (No. CityU 122612).

References

[1] D.S. Sadafule, S.P. Panda, Photocrosslinkable unsaturated polyesters, Journal of Applied Polymer Science 24 (1979) 511–521.
[2] B.K. Kandola, A.R. Horrocks, P. Myler, D. Blair, The effect of intumescents on the burning behavior of polyester–resin-containing composites, Composites Part A: Applied Science and Manufacturing 33 (2002) 805–817.
[3] S. Hörold, Phosphorus flame retardants in thermoset resins, Polymer Degradation and Stability 64 (1999) 427–431.
[4] S.Y. Lu, I. Hamerton, Recent developments in the chemistry of halogen-free flame retardant polymers, Progress in Polymer Science 27 (2002) 1661–1712.
[5] T.D. Hapuarachchi, T. Peijs, Aluminium trihydroxide in combination with ammonium polyphosphate as flame retardants for unsaturated polyester resin, eXPRESS Polymer Letters 3 (2009) 743–751.
[6] M.R. Ricciardi, V. Antonucci, M. Zarrelli, M. Giordano, Fire behavior and smoke emission of phosphate-based inorganic fire-retarded polyester resin, Fire and Materials 36 (2012) 203–215.
[7] C.M.C. Pereira, M. Herrero, F.M. Labajos, A.T. Marues, V. Rives, Preparation and properties of new flame retardant unsaturated polyester nanocomposites based on layered double hydroxides, Polymer Degradation and Stability 94 (2009) 939–946.
[8] S. Sen, Effect of both silane-grafted and ion-exchanged organophilic clay in structural, thermal, and mechanical properties of unsaturated polyester nanocomposites, Polymer Composites 31 (2010) 482–490.
[9] X.L. Chen, L.L. Huo, C.M. Jiao, S.X. Li, TG-FTIR characterization of volatile compounds from flame retardant polyurethane foams materials, Journal of Analytical and Applied Pyrolysis 100 (2013) 186–191.
[10] H.B. Chen, X. Dong, D.A. Schiraldi, L. Chen, D.Y. Wang, Y.Z. Wang, Phosphorus-containing poly(trimethylene terephthalate) derived from 2-(6-oxido-6H-dibenz ⟨c,e⟩ ⟨1,2⟩ oxaphosphorin-6-yl)-1,4-hydroxythoxy

phenylene: synthesis, thermal degradation, combustion and pyrolysis behavior, Journal of Analytical and Applied Pyrolysis 99 (2013) 40–48.
[11] C.Q. Yang, Q.L. He, Applications of micro-scale combustion calorimetry to the studies of cotton and nylon fabrics treated with organophosphorus flame retardants, Journal of Analytical and Applied Pyrolysis 91 (2011) 125–133.
[12] J. Artner, M. Ciesielski, O. Walter, M. Döring, R.M. Perez, J.K.W. Sandler, V. Altstädt, B. Schartel, A novel DOPO-based diamine as hardener and flame retardant for epoxy resin systems, Macromolecular Materials and Engineering 293 (2012) 503–514.
[13] Y.L. Liu, Epoxy resins from novel monomers with a bis-(9 10-dihydro-9-oxa-10-o-xide-10-phosphaphenanthrene-10-yl-) substituent, Journal of Polymer Science Part A: Polymer Chemistry 40 (2012) 359–368.
[14] R.M. Perez, J.K.W. Sandler, V. Altstädt, T. Hoffmann, D. Pospiech, M. Ciesielski, M. Döring, Effect of DOP-based compounds on fire retardancy, thermal stability, and mechanical properties of DGEBA cured with 4,4′-DDS, Journal of Materials Science 41 (2006) 341–353.
[15] B. Schartel, A.I. Balabanovich, U. Braun, U. Knoll, J. Artner, M. Ciesielski, M. Döring, R. Perez, J.K.W. Sandler, V. Altstädt, T. Hoffmann, D. Pospiech, Pyrolysis of epoxy resins and fire behavior of epoxy resin composites flame-retarded with 9,10-dihydro-9-oxa-10-phosphaphenanthrene-10-oxide additives, Journal of Applied Polymer Science 104 (2007) 2260–2269.
[16] R.M. Perez, J.K.W. Sandler, V. Altstädt, T. Hoffmann, D. Pospiech, M. Ciesielski, M. Döring, U. Braun, U. Knoll, B. Schartel, Effective halogen-free flame retardants for carbon fiber-reinforced epoxy composites, Journal of Materials Science 41 (2006) 4981–4984.
[17] C.S. Wu, Y.L. Liu, Y.S. Chiu, Epoxy resins possessing flame retardant elements from silicon incorporated epoxy compounds cured with phosphorus or nitrogen containing curing agents, Polymer 43 (2002) 4277–4284.
[18] X.D. Wang, Q. Zhang, Synthesis, characterization, and cure properties of phosphorus-containing epoxy resins for flame retardance, European Polymer Journal 40 (2004) 385–395.
[19] B. Perret, B. Schartel, K. Stöß, M. Ciesielski, J. Diederichs, M. Döring, J. Krämer, V. Altstädt, Novel DOPO-based flame retardant in high-performance carbon fiber epoxy composites for aviation, European Polymer Journal 47 (2011) 1081–1089.
[20] Y.Q. Xiong, Z.J. Jiang, Y.Y. Xie, X.Y. Zhang, W.J. Xu, Development of a DOPO-containing melamine epoxy hardeners and its thermal and flame-retardant properties of cured products, Journal of Applied Polymer Science 127 (2013) 4352–4358.
[21] B. Perret, B. Schartel, K. Stöß, M. Ciesielski, J. Diederichs, M. Döring, J. Krämer, V. Altstädt, A new halogen-free flame retardant based on 9,10-dihydro-9-oxa-10-phos-phaphenanthrene-10-oxide, Macromolecular Materials and Engineering 296 (2011) 14–30.
[22] D.C. Tahmassebi, T. Sasaki, Synthesis of a new trialdehyde template for molecular imprinting, The Journal of Organic Chemistry 59 (1994) 679–681.
[23] E. Kandare, B.K. Kandola, D. Price, S. Nazare, R.A. Horrocks, Study of the thermal decomposition of flame-retarded unsaturated polyester resins by thermogravimetric analysis and Py-GC/MS, Polymer Degradation and Stability 93 (2008) 1996–2006.
[24] W.Y. Xing, L. Song, P. Lv, G.X. Jie, X. Wang, X.Q. Lv, Y. Hu, Preparation, flame retardancy and thermal behavior of a novel UV-curable coating containing phosphorus and nitrogen, Materials Chemistry and Physics 123 (2010) 481–486.
[25] L. Yan, Y.B. Zheng, X.B. Liang, Q. Ma, Copolymerization of 1-Oxo-2,6,7-trioxa-1-phorsphabicyclo [2,2,2] oct-4-yl methyl acrylate and (10-oxo-10-hydro-9-oxa-10-phosphaphenanthrene-10-yl) methl acrylate with styrene and their thermal degradation characteristics, Journal of Applied Polymer Science 115 (2010) 1032–1038.
[26] R. Thangamani, T.V. Chinnaswamy, S. Palanichamy, A.W. Charles, HET acid based oligoesters-TGA/FTIR studies, European Polymer Journal 44 (2008) 1865–1873.
[27] H. Zhang, P.R. Westmoreland, F.J. Farris, E.B. Coughlin, A. Plichta, Z.K. Brzozowski, Thermal decomposition and flammability of fire-resistant, UV/visible-sensitive polyarylates, copolymers and blends, Polymer 43 (2002) 5463–5472.
[28] A.R. Tripathy, F. Farris, W.J. Macknight, Novel fire resistant matrixes for composites from cyclic poly(butylenes terephthalate), Polymer Engineering and Science 47 (2007) 1536–1543.
[29] R. Mosurkal, L.A. Samuelson, K.D. Smith, P.R. Westmoreland, V.S. Parmar, F. Yan, J. Kumar, A.C. Watterson, Nanocomposites of TiO_2 and siloxane copolymers as environmentally safe flame-retardant materials, Journal of Macromolecular Science Part A: Pure and Applied Chemistry 45 (2008) 942–946.
[30] H.Q. Zhang, R.J. Farris, P.R. Westmoreland, Low flammability and thermal decomposition behavior of poly (3,3′-dihydroxybiphenylisophthalamide) and its derivatives, Macromolecules 36 (2003) 3944–3954.
[31] B.B. Wang, X.F. Wang, G. Tang, Y.Q. Shi, W.Z. Hu, H.D. Lu, L. Song, Y. Hu, Preparation of silane precursor microencapsulated intumescent flame retardant and its enhancement on the properties of ethylene–vinyl acetate copolymer cable, Composites Science and Technology 72 (2012) 1042–1048.
[32] Q.L. Tai, Y. Hu, R.K.K. Yuan, L. Song, H.D. Lu, Synthesis, structure–property relationships of polyphosphoramides with high char residues, Journal of Materials Chemistry 21 (2011) 6621–6627.